

Magnetic properties of delta- and kagome-like chains with competing interactions

D. V. Dmitriev and V. Ya. Krivnov*

*Institute of Biochemical Physics of RAS,
Kosygin str. 4, 119334, Moscow, Russia.*

(Dated:)

We study the delta-chain with spin-1 on basal sites and spin- $\frac{1}{2}$ on apical sites. The Heisenberg interaction between neighbor basal spins is antiferromagnetic (AF) and the interaction between basal and apical spins is ferromagnetic (F). We show that the magnetization curve of this model is the same as that of the spin- $\frac{1}{2}$ kagome-like chain with competing Heisenberg interactions. The ground state phase diagram of the latter as a function of the ratio between the AF and F interaction, α , consists of the ferromagnetic, ferrimagnetic and singlet phases. We study the magnetic properties in each ground state phase and analyze the magnetization curves. We show that there are magnetization plateaus and jumps in definite regions of value α . We compare the magnetic properties of considered models with those of the spin- $\frac{1}{2}$ delta chain.

I. INTRODUCTION

Low-dimensional quantum magnets based on a geometrically frustrated lattice are of considerable interest from both experimental and theoretical points of view [1, 2]. One of the typical example of these systems is the delta or the sawtooth chain, i.e. the Heisenberg model on a linear chain of triangles, as shown in Fig.1. The Hamiltonian of this model has the form

$$\hat{H} = J_1 \sum_{i=1}^N (\mathbf{S}_{i-1} + \mathbf{S}_i) \cdot \sigma_i + J_2 \sum_{i=1}^N \mathbf{S}_{i-1} \cdot \mathbf{S}_i - h \sum_{i=1}^N (S_i^z + \sigma_i^z) \quad (1)$$

where σ_i and \mathbf{S}_i are the apical and the basal spin operators with spin quantum numbers s_a and s_b , correspondingly. The interaction J_1 acts between apical and basal spins, while J_2 is

*Electronic address: krivnov@deom.chph.ras.ru

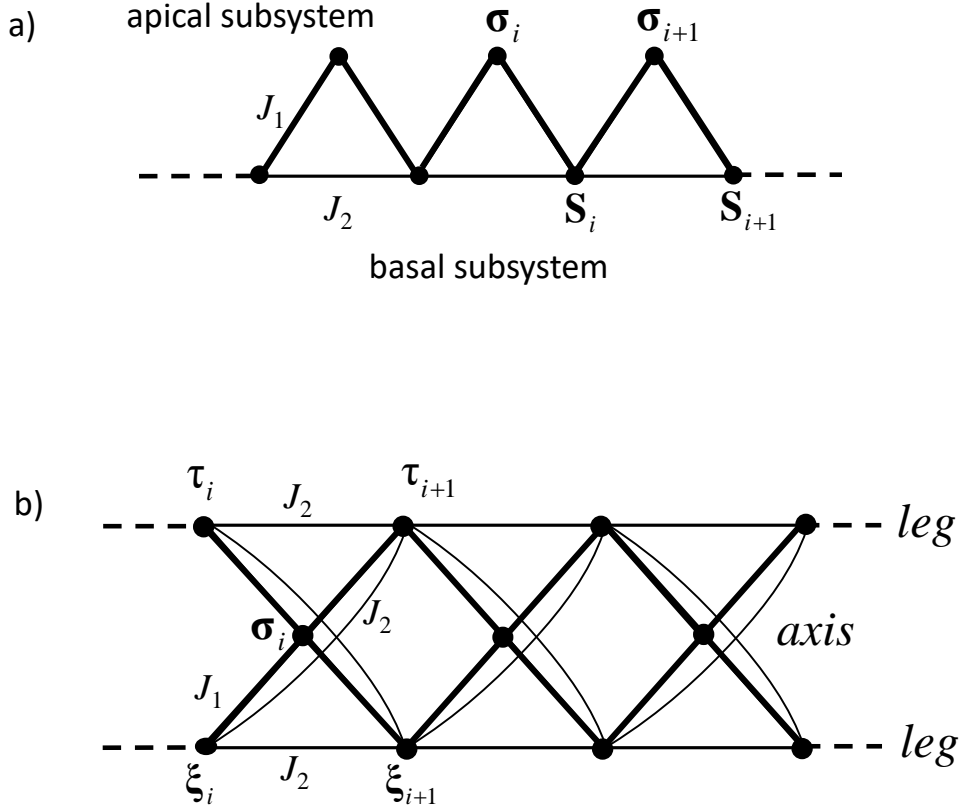


FIG. 1: Delta-chain (a) and kagome chain (b) spin models.

the interaction between neighbor basal spins. The direct exchange between apical spins is absent, h is dimensionless magnetic field and N is number of triangles in the cyclic system.

A quantum delta chain with both antiferromagnetic interactions, $J_1 > 0$ and $J_2 > 0$ is well studied [3–11] and has a number of interesting properties. At the same time, the delta chain with the ferromagnetic J_1 and antiferromagnetic J_2 interactions (F-AF delta-chain) is very interesting as well and has attracted interest last time. The $s = \frac{1}{2}$ F-AF delta-chain (with both $s_a = s_b = \frac{1}{2}$) is a minimal model describing real compounds, in particular, malonate-bridged copper complexes [12–15] and new kagome fluoride $Cs_2LiTi_3F_{12}$ in which the delta-chains host as magnetic subsystems [16]. Another very interesting example of the F-AF delta-chain compound is recently synthesized cyclic complexes $Fe_{10}Gd_{10}$ with Gd and Fe ions as the apical and basal spins with $s_a = \frac{7}{2}$ and $s_b = \frac{5}{2}$, correspondingly [17].

Of particular interest is the study of the magnetic properties of the F-AF model depending on the value of the frustration parameter $\alpha = \frac{J_2}{|J_1|}$. The ground state of this model is ferromagnetic for $\alpha < \frac{s_a}{2s_b}$. The value $\alpha_c = \frac{s_a}{2s_b}$ corresponds to the quantum critical point

separating the ground state phases. The properties of the F-AF delta-chain in the critical point are highly nontrivial. As it is shown in [18–22] the ground state consists of localized magnons and bound magnon complexes which form macroscopically degenerate ground state manifold. The total number of the ground states is [18]:

$$G(N) = 2^N + 2N(s_a + s_b - \frac{1}{2})C_N^{N/2} \quad (2)$$

As a consequence the residual entropy per triangle is $\mathcal{S} = \ln 2$ at zero temperature.

The magnetization curve calculated with partition function accounting only ground state manifold in the limit $h \gg T/N$ has a form [18]

$$M = [s_a + s_b - \frac{1}{1 + e^{h/T}}]N \quad (3)$$

As follows from Eq.(3) the magnetization per triangle $m = \frac{M}{N}$ at $\frac{h}{T} \rightarrow 0$ tends to $m = (s_a + s_b - \frac{1}{2})$. Therefore, the F-AF delta chain is magnetically ordered at zero temperature in the critical point and the magnetization undergoes a jump from $m = (s_a + s_b)$ in the ferromagnetic phase to $m = (s_a + s_b - \frac{1}{2})$ at the critical point.

As we noted before the critical point separates different ground state phases. One of them is ferromagnetic at $\alpha < \alpha_c$. The question arises about a nature of the ground state and the magnetic properties of the F-AF delta-chain at $\alpha > \alpha_c$ and their dependence on spin values s_a and s_b . For example, the $s = \frac{1}{2}$ F-AF delta chain has the ferrimagnetic ground state in the whole region $\alpha > \alpha_c$ as it was shown in [23, 24] on the base of numerical calculations. But the structure of this state is not quite clear especially for $\alpha \gg 1$.

In this paper we consider another example of the F-AF delta-chain consisting of spins with $s_a = \frac{1}{2}$ and $s_b = 1$. As it will be seen from the following this model has more complex ground state phase diagram at $\alpha > \alpha_c$ ($\alpha_c = \frac{1}{4}$) in contrast with the $s = \frac{1}{2}$ F-AF model. It is interesting to note that considered delta-chain is closely related to another model with competing F and AF interactions, which is kagome-like spin- $\frac{1}{2}$ chain shown in Fig.1b. The Hamiltonian of the latter has a form

$$\hat{H} = J_1 \sum_{i=1}^N (\tau_i + \xi_i) \cdot (\sigma_{i-1} + \sigma_i) + J_2 \sum_{i=1}^N (\tau_i + \xi_i) \cdot (\tau_{i+1} + \xi_{i+1}) \quad (4)$$

where σ_i , τ_i and ξ_i are $s = \frac{1}{2}$ operators of spins on axis, upper and lower legs, respectively (see Fig.1b). The axis-leg interaction J_1 is ferromagnetic and leg-leg interaction J_2 is antiferromagnetic. (We further put $J_1 = -1$ and $J_2 = \alpha$).



FIG. 2: The phase diagram of delta and kagome chain models.

Model (4) describes an interesting class of quasi-one-dimensional compounds $Ba_3Cu_3In_4O_{12}$ and $Ba_3Cu_3Sc_4O_{12}$ [25–27].

It is remarkable that the ground state phase diagram of the F-AF delta-chain, with $s_a = \frac{1}{2}$, $s_b = 1$ is the same as that for the F-AF kagome chain (4). This conclusion follows from the comparison of basis states of both models. The spins τ_i and ξ_i on i -th sites of kagome legs are incorporated into the compound spin $(\tau_i + \xi_i)$ which is either 1, or 0. Thus, the kagome chain (4) is equivalent to such delta-chain in which each basal site can be occupied by spin 1 or spin 0. The site with spin 0 is really empty (defect) site because its spin does not interact with neighbor basal spins 1 and apical spins $\frac{1}{2}$, i.e. such sites separate the delta-chain into an ensemble of finite chain fragments decoupled from each other. It is easy to check that the state with the lowest energy for given S does not contain spin 0 sites, because each defect increases the energy by the value $\Delta E \simeq 2|\varepsilon(S)|$, where $\varepsilon(S)$ is the ground state energy per triangle. Therefore, the ground states of the kagome chain (4) and the F-AF delta chain with $s_a = \frac{1}{2}$ and $s_b = 1$ coincide in each spin sector for all values of α and the magnetization at $T = 0$ is the same for both models. As it was shown in [20] the ground state degeneracy at the critical point $\alpha_c = \frac{1}{4}$ is the same for both models and it is given by (2). The ground state phase diagram of the kagome chain (4) was determined by T. Yamaguchi, Y. Ohta, and S. Nishimoto in Ref.[28]. According to results of [28] both models have five ground state phases as it is shown in Fig.2. At $\alpha < \frac{1}{4}$ the ground state is ferromagnetic and the magnetization undergoes a jump from $m = \frac{3}{2}$ in the ferromagnetic phase to $m = 1$ at the critical point α_c . The phases in regions $0.25 < \alpha < 0.33$ and $0.42 < \alpha < 0.6$ are ferrimagnetic but with different ground state spins, and the ground state is the singlet in regions $0.33 < \alpha < 0.42$ and $\alpha > 0.6$.

In the present paper we consider the magnetic properties in each phase and study the zero-temperature magnetization processes in them. We will show that the properties of the considered models at $\alpha > \alpha_c$ are essentially different from those for the $s = \frac{1}{2}$ delta-chain.

In particular, this concerns the region of large α where these models have different ground states and different behavior of the magnetization. In order to study the ground state and the spectrum of the delta-chain with $s_a = \frac{1}{2}$ and $s_b = 1$ we employ analytical approaches and exact diagonalization (ED) and DMRG numerical calculations.

The paper is organized as follows. In Section II we consider the magnetic properties of the F-AF model in the ferrimagnetic phase Ferri1. We give an analytical estimate of the magnetization $m(h)$ and compare it with numerical results. In Section III we study the magnetization in an intermediate singlet phase and show that jumps in the magnetization curve occur in this phase. In Section IV we consider the ferrimagnetic phase Ferri 2 in which the magnetization curve has a plateau. In Section V we study the magnetization in the singlet phase at $\alpha > 0.6$. In the region $0.6 < \alpha < 2$ the magnetization jump occurs and at $\alpha > 2$ the magnetization curve has a plateau. In this section we also compare the behavior of the considered models with that for the F-AF $s = \frac{1}{2}$ delta-chain at $\alpha \gg 1$. In Section VI we give a summary.

II. VICINITY OF THE CRITICAL POINT $0.25 < \alpha < 0.33$

For $\alpha > \frac{1}{4}$ the macroscopic ground state degeneracy (2) splits. At small value of γ ($\gamma = \alpha - \frac{1}{4}$) the total spin of the ground state S_{tot} is close to N . The numerical calculations of finite chains give $S_{tot} = N$ for $N < 12$, $S_{tot} = N + 1$ for $12 \leq N < 30$ and $S_{tot} = N + 2$ for $N = 30$ at $\gamma = 0.01$. It is unclear from these numerical data whether the excess over $S_{tot} = N$ is thermodynamic or it vanishes in the thermodynamic limit. To answer this question and determine the value of the total spin of the ground state in the thermodynamic limit, we study the behavior of the magnetization curve, $m(h)$.

At first we consider the behavior of $m(h)$ near the saturation field $h = h_s$. Above the saturation field the system is, ferromagnetically ordered. Below h_s the model is described in terms of down spins (magnons) on the ferromagnetic background. The saturation field is equal to a minimal energy of the one-magnon state which is $E_1 = -4\gamma$, i.e. $h_s = 4\gamma$.

The system of magnons near h_s can be considered as the Bose-gas with the δ -function interaction, which at low density is equivalent to spinless fermions [29–31]. Spin operators of basal spin-1 \mathbf{S}_n and apical spin- $\frac{1}{2}$ σ_n in the fermion representation are:

$$S_n^+ = \sqrt{2}b_n, \quad S_n^z = 1 - b_n^+b_n \quad (5)$$

$$\sigma_n^+ = a_n, \quad \sigma_n^z = \frac{1}{2} - a_n^+ a_n \quad (6)$$

Then the Hamiltonian takes the form:

$$\begin{aligned} \hat{H}_f = & E_F - \frac{1}{\sqrt{2}} \sum_{n=1}^N [b_n^+ (a_n + a_{n-1}) + (a_n^+ + a_{n-1}^+) b_n] + \\ & + \alpha \sum_{n=1}^N (b_n^+ b_{n+1} + b_{n+1}^+ b_n) + (1 - 2\alpha) \sum_{n=1}^N b_n^+ b_n + 2 \sum_{n=1}^N a_n^+ a_n \end{aligned} \quad (7)$$

where $E_F = (\alpha - 1)N$ is the energy of the ferromagnetic state. Near h_s the number of fermions is small and we ignored in \hat{H}_f four-fermion terms.

Diagonalizing the Hamiltonian \hat{H}_f , we arrive at

$$\hat{H}_f = E_F + \sum_k E_-(k) A_k^+ A_k + \sum_k E_+(k) B_k^+ B_k \quad (8)$$

where A_k and B_k are new Fermi-operators and the spectrum $E_{\pm}(k)$ is

$$E_{\pm}(k) = \frac{3}{2} - \alpha(1 - \cos k) \pm [(\frac{1}{2} + \alpha(1 - \cos k))^2 + (1 + \cos k)]^{1/2} \quad (9)$$

$E_-(k)$ is the lowest branch and its minimum is $E_-(k = \pi) = -4\gamma$. The z -projection of total spin S^z is given by

$$S^z = \frac{3N}{2} - \sum_k (A_k^+ A_k + B_k^+ B_k) \quad (10)$$

At magnetic field close to the saturated value, the number of fermions is small and we fill the lowest branch $E_-(k)$ in the momentum space region $[\pi - k_F, \pi + k_F]$. Then the energy in the magnetic field h becomes

$$E = E_F + \frac{N}{\pi} \int_{\pi - k_F}^{\pi} E_-(k) dk - h S^z \quad (11)$$

where

$$S^z = \frac{3N}{2} - N \frac{k_F}{\pi} \quad (12)$$

The dependence $m(h)$ is obtained from the condition $\frac{dE}{dk_F} = 0$, which leads to the equation for $k_F(h)$:

$$E_-(\pi - k_F) + h = 0 \quad (13)$$

When h is close to h_s , the value of $k_F \ll 1$ and the leading term for $m(h)$ is

$$m = \frac{3}{2} - \frac{2\sqrt{2}\sqrt{1+2\gamma}}{\pi\sqrt{3+4\gamma}} \sqrt{1 - \frac{h}{h_s}} \quad (14)$$

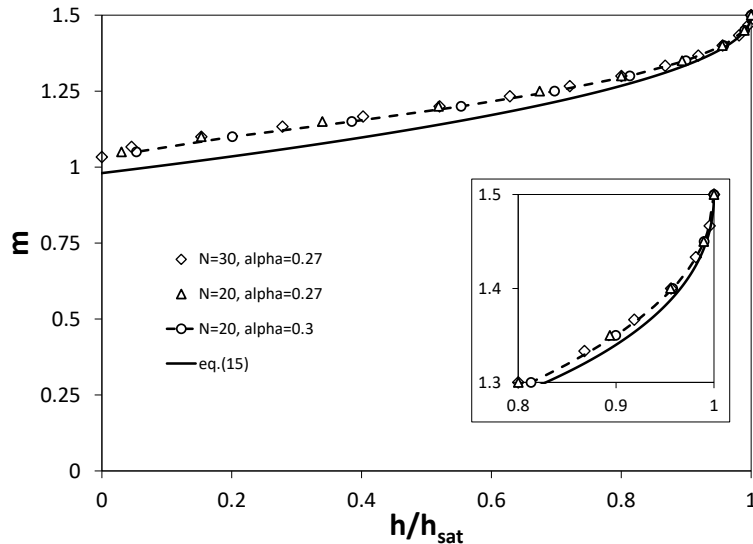


FIG. 3: Magnetization curve near the transition point. The inset shows the behavior of the magnetization curve near the saturation field.

As it is known [32, 33] the magnetization curve near h_s can be constructed with the use of the solution of two-magnon problem. Our consideration of the state with $S^z = \frac{3N}{2} - 2$ shows that the leading term of $m(h)$ for $(h_s - h) \ll h_s$ coincides with Eq.(14).

If $\gamma \ll 1$ then $m(h)$ is

$$m = \frac{3}{2} - b\sqrt{1 - \frac{h}{h_s}} \quad (15)$$

where $b = \frac{2}{\pi}\sqrt{\frac{2}{3}} \approx 0.52$.

Though Eq.(15) is valid for h close to h_s , it turns out that this estimate gives reasonable accuracy up to the case $h = 0$. In Fig.3 numerical calculations (DMRG) of the magnetization curve for $N = 20, 30$ and $\alpha = 0.27, 0.3$ are compared with Eq.(15). As it is seen on the inset of Fig.3, Eq.(15) perfectly describes the numerical results near the saturation field. For low and intermediate values of the magnetic field, the analytical estimate (15) slightly diverges from the numerical results and, finally, Eq.(15) predicts the total spin of the ground state $S_{tot} \simeq 0.98N$ at $h = 0$. At the same time, the numerical calculations shown in Fig.3 indicate that all magnetization curves for different N are very close to each other and all of them tends to the same value $S_{tot} \simeq 1.04N$ at $h \rightarrow 0$. Thus, the small excess of the total spin of the

ground state over $S_{tot} = N$ detected on finite chains does not vanish in the thermodynamic limit and leads to an increase of S_{tot} by 4%.

The case when all spins of the delta-chain (both apical and basal) are $s_a = s_b = \frac{1}{2}$ can be also studied in terms of the fermion representation of magnons. The leading term for the magnetization $m(h)$ near the saturation field $h_s = 2\gamma$ ($\gamma = \alpha - \frac{1}{2}$) has a form

$$m = 1 - \frac{\sqrt{2}\sqrt{1+2\gamma}}{\pi\sqrt{1+\gamma}} \sqrt{1 - \frac{h}{h_s}} \quad (16)$$

Eq.(16) gives the estimate for the total spin of the ground state $S_{tot} \simeq 0.55N$ ($\gamma \ll 1$) at $h = 0$, which is in very good agreement with the ground state spin $S_{tot} \simeq 0.54N$ obtained by numerical calculations [24]. Therefore, the value of $S_{tot} \simeq 0.54N$ in the $s_a = s_b = \frac{1}{2}$ delta chain model slightly exceeds the value of magnetization $S_{tot} = 0.5N$ at the critical point. This fact is in accord with the studied models, where the ground state total spin $S_{tot} \simeq 1.04N$ is slightly above the value of the magnetization at the critical point $M = N$.

III. INTERMEDIATE SINGLET PHASE $0.33 < \alpha < 0.43$

Intermediate singlet phase is realized in the region $0.33 < \alpha < 0.43$. The singlet ground state has a period 6 [28], so that the periodic chains of length $N = 6k$ have singlet ground states, while systems of other lengths have ground states with non-zero total spin S_{tot} , which is however vanishing in the thermodynamic limit $N \rightarrow \infty$. The magnetization curve for $\alpha = 0.4$ is shown in Fig.4 for $N = 18, 24$. As it is seen in Fig.4 the magnetization curve has two magnetization jumps, the first one occurs at $h_1 \simeq 0.0036$ from the singlet state to $S_{tot} = N/2$, then after magnetization plateau at $m = \frac{1}{2}$, the second jump takes place at $h_2 \simeq 0.0285$ from $m = \frac{1}{2}$ to the value slightly lower than $m = 1$.

Both fields h_1 and h_2 tend to zero when $\alpha \rightarrow 0.33$, providing the phase transition to the ferrimagnetic ground state with $S_{tot} \simeq 1.04N$. On the other side of the region, $\alpha \rightarrow 0.43$, the transition to another ferrimagnetic phase with $S_{tot} = N/2$ takes place, as will be shown in the next section. Therefore, the first field h_1 vanishes at the phase boundary $\alpha = 0.43$, while the second magnetization jump continuously transform to the steep square-root behavior of $m(h)$ above $m = \frac{1}{2}$ in the ferrimagnetic region $0.43 < \alpha < 0.6$.

The plateau at $m = 0$ shown in Fig.4 for $N = 18, 24$ at first glance contradicts to the numerical results of zero singlet-triplet energy gap presented in Fig.5 of Ref.[28]. However,

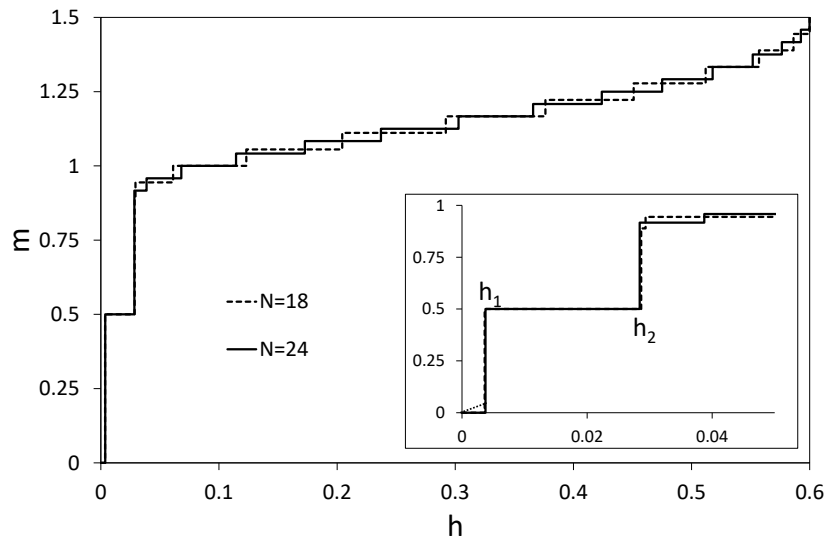


FIG. 4: Magnetization curve for $\alpha = 0.4$ and $N = 18, 24$. The inset shows the low magnetic field part of the magnetization curve.

this is just finite-size effect, that is the value of $h_1 \simeq 0.0036$ is so low, that to observe the first step on the magnetization curve (at h equal to the singlet-triplet gap) one need to calculate the chains much longer than $N = 24$. So that in the thermodynamic limit there is an approximately linear growth of magnetization in the region $0 < h < h_1$, which we indicated by dotted line in Fig.4.

IV. FERRIMAGNETIC PHASE $0.43 < \alpha < 0.6$

When $\alpha > 0.43$, the total spin of the ground state changes from $S_{tot} = 0$ to $S_{tot} = N/2$ [28]. The dependence $E(S_{tot})$ in this region is very flat for $S_{tot} \leq N/2$, so that the energy difference is negligible in the thermodynamic limit, and ground state is quasi-degenerate with $0 \leq S_{tot} \leq N/2$. The example of the dependence $E(S_{tot})$ is presented in Fig.5 for $N = 8$.

The ferrimagnetic phase in this region is accompanied by the energy gap for the states with $S_{tot} = N/2 + 1$, which manifests itself in the plateau at $m = \frac{1}{2}$ on the magnetization curve. The numerical data confirms these facts. The magnetization curve for $N = 16$

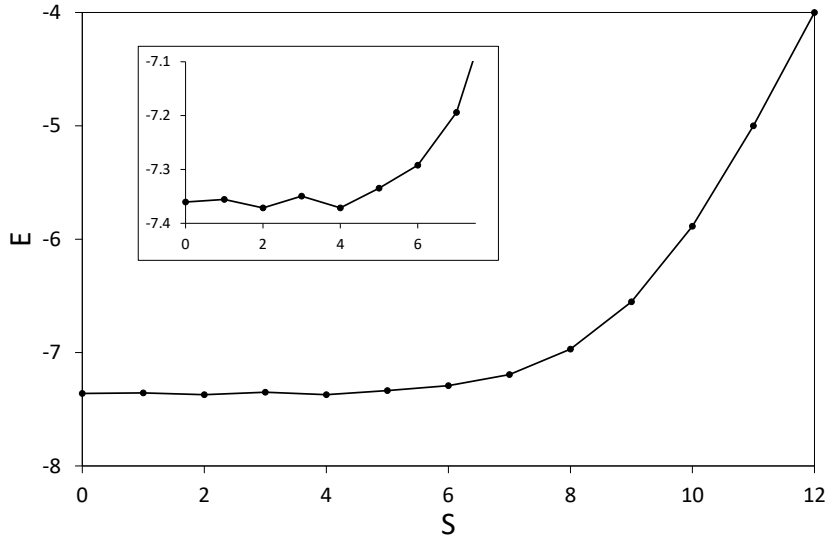


FIG. 5: Spectrum $E(S)$ for $\alpha = 0.5$ and $N = 8$. The inset shows the low energy part of $E(S)$.

at $\alpha = 0.5$ is shown in Fig.6. One can see the plateau at $m = \frac{1}{2}$ up to the magnetic field $h_{up} \simeq 0.031$, which is in accord with the numerical data for the energy gap shown in Fig.2 of Ref.[28]. Above h_{up} the magnetization curve shows square-root-like behavior $m - \frac{1}{2} \sim \sqrt{h - h_{up}}$. Similar square-root behavior occurs near the saturation field, where $\frac{3}{2} - m \sim \sqrt{h_s - h}$.

The case $\alpha = 0.5$ is a generic case for the region $0.43 < \alpha < 0.6$, so that the behavior of the system in the whole region is similar to the case $\alpha = 0.5$.

V. SINGLET PHASE $\alpha > 0.6$

We start to study the singlet phase $\alpha > 0.6$ from the limit $\alpha \gg 1$. When $\alpha = \infty$ the model consists of two non-interacting subsystems: the basal antiferromagnetic chain and isolated apical spins. For large but finite α the interaction between two subsystems can be treated in the frame of the perturbation theory (PT) in small parameter $\frac{1}{\alpha}$. In this limit it is convenient to renormalize the interactions as $J_2 = 1$ and $J_1 = -\frac{1}{\alpha}$ and the Hamiltonian (1) takes the form

$$\hat{H} = \hat{H}_0 + \hat{V} \quad (17)$$

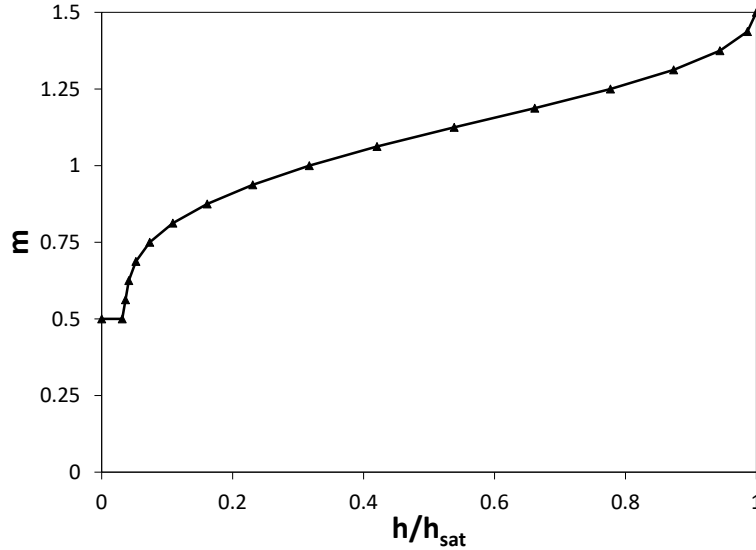


FIG. 6: Magnetization curve for $\alpha = 0.5$ and $N = 16$.

$$\hat{H}_0 = \sum \mathbf{S}_i \cdot \mathbf{S}_{i+1} \quad (18)$$

$$\hat{V} = -\frac{1}{\alpha} \sum (\mathbf{S}_{i-1} + \mathbf{S}_i) \cdot \sigma_i \quad (19)$$

where \hat{H}_0 is the Hamiltonian of the antiferromagnetic basal chain and \hat{V} is the basal-apical interaction.

The ground state of \hat{H}_0 is a singlet and by its symmetry the first order in \hat{V} is zero. However, in the triplet state of basal subsystem the first order of PT is nonzero and $\langle \hat{V} \rangle$ is

$$\langle \hat{V} \rangle = -\frac{1}{\alpha} \sum \langle S_i^z + S_{i+1}^z \rangle \sigma_i^z \quad (20)$$

The average $\langle S_i^z + S_{i+1}^z \rangle$ in the triplet state is $\langle S_i^z + S_{i+1}^z \rangle = \frac{2}{N}$ (PBC is assumed) and $\langle \hat{V} \rangle$ has the minimum when all $\sigma_i^z = \frac{1}{2}$, i.e. the apical subsystem is fully polarized, so that the total spin of the system is $S_{tot} = \frac{N}{2} + 1$ ($S = S_a + S_b$). The energy of the lowest triplet of \hat{H}_0 (the singlet-triplet gap) is $\Delta_1 = 0.4105$ [34]. Therefore, in the first order of PT the energy of the state with $S_{tot} = \frac{N}{2} + 1$ (the basal triplet and the fully polarized apical subsystem) is

$$E_1 = E_0 + \left(\Delta_1 - \frac{1}{\alpha}\right) \quad (21)$$

where $E_0 = -1.41N$ [34]. Therefore, for $\alpha \gg 1$ the state with $S_{tot} = \frac{N}{2} + 1$ can not be

the ground state, because the small apical-basal interaction can not overcome the finite singlet-triplet gap in the basal subsystem.

As we noted before, the first order PT in $\frac{1}{\alpha}$ for the singlet ground state of \hat{H}_0 is zero and, therefore, independent of the apical subsystem configuration. In order to determine the ground state of the apical subsystem we need to study the next order of PT. The second order PT for the singlet ground state of the basal subsystem leads to an effective spin- $\frac{1}{2}$ Hamiltonian for the apical subsystem, as it was shown in Ref.[35]. Though the basal-apical interaction in the model studied in Ref.[35] is AF, the sign of this interaction is unimportant in the second order PT in $\frac{1}{\alpha}$ and the results of [35] are applicable to the present model. The effective Hamiltonian describing the apical subsystem is rather unusual. It represents two weakly interacting and frustrated spin- $\frac{1}{2}$ Heisenberg spin-chains on odd and even apical sites. The ground state of this effective Hamiltonian is the singlet and the lowest energy $E(S_a)$ of the state with the total apical spin S_a is a smoothly increasing function up to $S_a = \frac{N}{2}$ with a small prefactor α^{-2} .

Based on the above we can describe the behavior of the system in the external magnetic field. At zero magnetic field the ground state of the model is the singlet consisting of both basal and apical singlets. For very low magnetic fields $h \sim \alpha^{-2}$ the apical subsystem becomes partly polarized, while the basal subsystem is in its singlet state. The magnetization per triangle $m = S_{tot}/N$ smoothly increases with h and the dependence $m(h)$ is governed by the function $E(S_a)$. At some "apical saturation field" h_{low} , the apical subsystem becomes fully polarized and $m = \frac{1}{2}$. Using the parameters of the effective Hamiltonian given in [35] we estimate this field as $h_{low} \approx 0.26/\alpha^2$. The magnetization curve $m(h)$ is steadily increases in the region $0 \leq h \leq h_{low}$ and $m(h)$ near h_{low} behaves as $m(h) \sim \frac{1}{2} - \sqrt{1 - \frac{h}{h_{low}}}$.

Further increase of the magnetic field $h > h_{low}$ does not lead to increase of the magnetization, providing a magnetization plateau at $m = \frac{1}{2}$, until the magnetic field overcomes the singlet-triplet gap of the basal subsystem. The state with $S = \frac{N}{2} + 1$ is represented in the first order PT as the lowest basal triplet in the field $h + \frac{1}{\alpha}$ formed by the polarized apical spins and external magnetic field. The energy of this state is given by Eq.(21) and it determines the field $h_{up} = (\Delta_1 - \frac{1}{\alpha})$ at which the magnetization starts to increase from the plateau at $m = \frac{1}{2}$. The difference $h_{up} - h_{low}$ is a width of the plateau of the magnetization at $m = \frac{1}{2}$. The states with $S > \frac{N}{2} + 1$ can be considered in the first order PT as the spin-1 Heisenberg basal chain in the magnetic field $h + \frac{1}{\alpha}$. The behavior of $E(S)$ near $S \geq \frac{N}{2}$ is

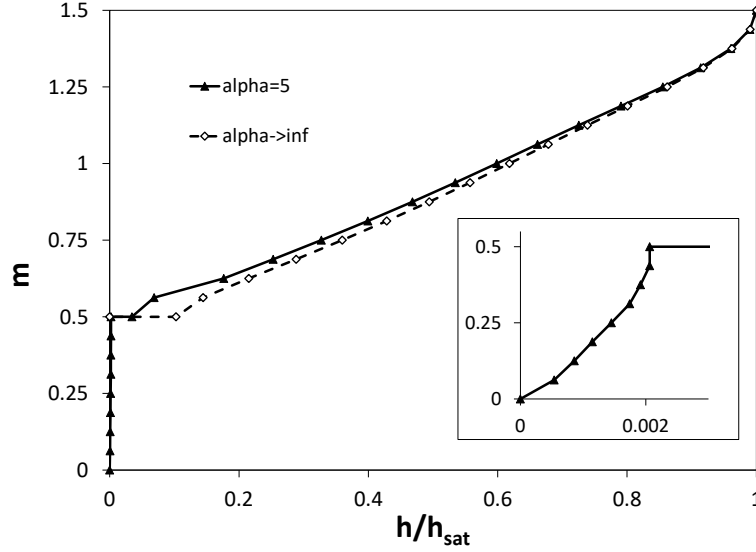


FIG. 7: Magnetization curve for $\alpha = 5$ and $N = 16$. The inset shows the low magnetic field part of the magnetization curve.

the same as that for the spin-1 Heisenberg chain [30]

$$E(S_b) = \Delta_1 S_b + d \frac{S_b^3}{N^2} \quad (22)$$

where $d \simeq 25$. This leads to the following behavior of the magnetization curve $m(h)$ near h_{up} :

$$m = \frac{1}{2} + 0.115 \sqrt{h - h_{up}} \quad (23)$$

Further strengthening of the magnetic field from h_{up} to $h_{sat} = 4\gamma$ results in the continuous increase of the magnetization and near h_{sat} the magnetization behaves as

$$m = \frac{3}{2} - \frac{4}{\pi} \sqrt{1 - \frac{h}{h_{sat}}} \quad (24)$$

The numerical calculations confirm the above reasoning. The magnetization curve for $\alpha = 5$ is shown in Fig.7 in comparison with the case $\alpha \rightarrow \infty$. As it is seen in Fig.7 both magnetization curves have plateau at $m = \frac{1}{2}$. In the inset of Fig.7 the behavior of the magnetization curve is shown for low magnetic field, where the magnetization occurs on the apical subsystem only.

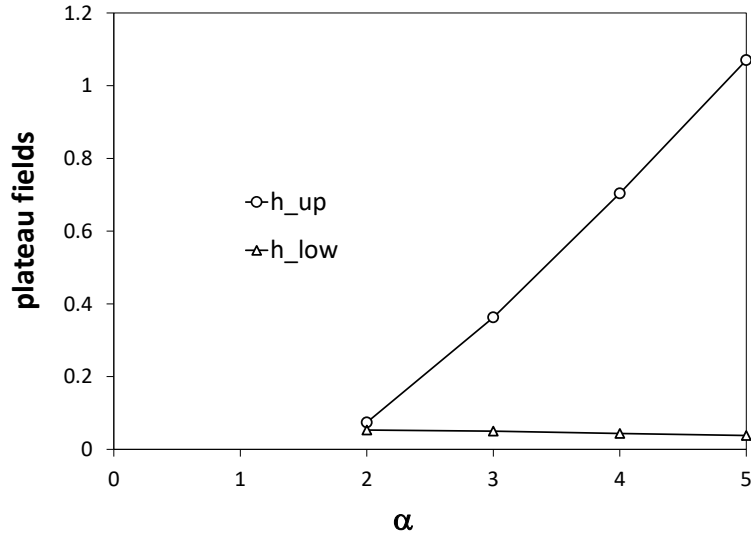


FIG. 8: Dependence of up and low magnetic fields, determining the magnetization plateau, on α .

The dependencies of h_{up} and h_{low} on α are shown in Fig.8. As follows from Fig.8 the plateau vanishes at some value of α slightly lower than $\alpha = 2$. It means that for $\alpha < 2$ the above speculative separation of the system on almost independent apical and basal subsystems is no longer relevant. The behavior of the magnetization curve in Fig.9 for $\alpha = 1$ indicates that after the vanishing of the plateau the metamagnetic jump at $h = h_{jump}$ is forming from some finite value $m_1 < \frac{1}{2}$ to the value m_2 close to $m = \frac{1}{2}$. When α decreases, h_{jump} decreases also and $h_{jump} \rightarrow 0$ when $\alpha \rightarrow 0.6$, so that the jump occurs from $m_1 \rightarrow 0$ to $m_2 \rightarrow \frac{1}{2}$. Finally, at $\alpha = 0.6$ the transition from the singlet phase to the ferrimagnetic phase with $m = \frac{1}{2}$ occurs.

Now let us compare the behavior of the considered models with that of spin- $\frac{1}{2}$ F-AF delta-chain in the $\alpha \gg 1$ limit. The main difference stems from different spectra of the basal AF chains: the gapped one for spin-1 and gapless for spin- $\frac{1}{2}$. The energy of the lowest triplet of \hat{H}_0 for the case $s_b = \frac{1}{2}$ is $\Delta E = \pi^2/N$. In the first order of PT (20) the energy difference between the states with $S_{tot} = \frac{N}{2} + 1$ (the basal triplet and fully polarized apical subsystem) and $S_{tot} = 0$ (the basal singlet and non-magnetic apical subsystem) is

$$E(S = \frac{N}{2} + 1) - E(S = 0) = \frac{\pi^2}{N} - \frac{1}{\alpha} \quad (25)$$

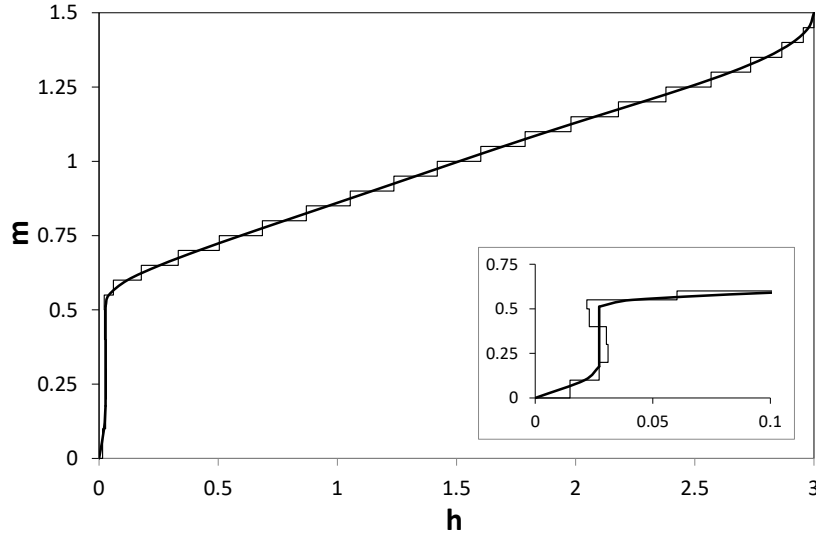


FIG. 9: Magnetization curve for $\alpha = 1$ and $N = 20$. The inset shows the low magnetic field part of the magnetization curve. The S-shaped form of the magnetization curve constructed as $h(S) = E(S + 1) - E(S)$ (thin lines) indicates the concavity of the dependence $E(S)$ and the corresponding jump in magnetization (thick line).

So, the state with $S_{tot} = \frac{N}{2} + 1$ has lower energy for $N > \pi^2\alpha$. The numerical value of $\pi^2\alpha$ is large, so one should be careful when interpreting the results of numerical calculations of finite chains. For example, for the delta-chain with $\alpha = 10$ the magnetic state with $S_{tot} = \frac{N}{2} + 1$ is realized for $N > 100$, while for $N < 100$ one observe the singlet ground state.

If we study the delta-chain of macroscopical size, we should examine the starting states of the basal subsystem with different macroscopical value of the total spin $S_b \sim N$ and their energies are [36]

$$E_b(S) = E_{0b} + \frac{\pi^2 S_b^2}{2N} \quad (26)$$

where $E_{0b} = (\frac{1}{4} - \ln 2)N$.

Taking into account the first order of PT (20) the energy of the total system becomes

$$E(S) = E_{0b} + \frac{\pi^2 S_b^2}{2N} - \frac{S_b}{\alpha} \quad (27)$$

Minimization of (27) over S_b gives $S_b = N/\pi^2\alpha$. Thus, the ground state for large α is ferrimagnetic with total spin $S_{tot} = N (\frac{1}{2} + \frac{1}{\pi^2\alpha})$.

The magnetization as a function of the external field h , rises continuously from the value

$$m = \frac{1}{2} + \frac{1}{\pi^2 \alpha} \quad (28)$$

at $h = 0$ to $m = 1$ at the saturation field $h_s = 2\alpha - 1$. We stress that the obtained magnetization (28) exceeds the value $m = \frac{1}{2}$ by a small, but finite value, describing the weak induced polarization of the basal subsystem. Near the saturation field the magnetization shows a common square root behavior: $1 - m \sim \sqrt{h_s - h}$.

Hence, the ground state of model (1) with basal spin-1 and spin- $\frac{1}{2}$ in the $\alpha \gg 1$ limit are different - singlet ground state for basal spin-1 and ferrimagnetic ground state with magnetization slightly higher than $m = \frac{1}{2}$ for basal spin- $\frac{1}{2}$. We expect that such difference remains for all other values of basal spins: singlet ground state for integer values of basal spins and ferrimagnetic ground state for half-integer values of basal spins.

VI. SUMMARY

We have studied the magnetic properties of the frustrated model consisting of the triangles with competing ferromagnetic interactions between basal spins-1 and apical spins- $\frac{1}{2}$ and antiferromagnetic interactions between basal spins. The magnetic properties of this model at zero temperature exactly coincides with that of the kagome-like spin- $\frac{1}{2}$ chain.

The ground state of these models depend on the ratio between antiferromagnetic and ferromagnetic interactions, α , and contains 5 phases: the ferromagnetic phase $\alpha < 0.25$; the ferrimagnetic phase ($m = 1.04$) $0.25 < \alpha < 0.33$; the intermediate singlet phase $0.33 < \alpha < 0.43$; the ferrimagnetic phase ($m = 0.5$) $0.43 < \alpha < 0.6$; the singlet phase $\alpha > 0.6$. We studied the magnetization curve in all these phases and found very specific evolution of the magnetization curve.

1) In the vicinity of the critical point ($0.25 < \alpha < 0.33$), the ground state has a total spin $S_{tot} = 1.04N$ and the magnetization smoothly increases with the magnetic field from $m = 1.04$ and tends to saturation $m = 3/2$ by a square-root law.

2) When $0.33 < \alpha < 0.43$ the ground state is singlet and the magnetization starts to increase from zero value. At some low value of the magnetic field h_1 the magnetization abruptly jumps to $m = 1/2$, then after plateau on the level $m = 1/2$ at h_2 the magnetization undergoes one more jump to the value slightly lower than $m = 1$. After the second jump

the magnetization smoothly increases to the saturation.

3) When $0.43 < \alpha < 0.6$, $h_1 = 0$ and the first magnetization jump disappears, so that the magnetization starts at $m = 1/2$. The plateau on the level $m = 1/2$ remains, but the magnetization jump at $h = h_2$ transforms to the sharp square-root increase of the magnetization curve for $h > h_2$.

4) When $\alpha > 0.6$, the ground state becomes singlet and the magnetization curve begins from $m = 0$. In the region $0.6 < \alpha < 2$ after short almost linear section $m \sim h$, the magnetization undergoes a jump at some field h_{jump} to a value close to $m = 1/2$. For $h > h_{jump}$ the magnetization gradually increases to the saturation. At a certain value of $\alpha \lesssim 2$, the magnetization jump disappears, and instead the magnetization plateau appears at the level $m = 1/2$.

5) Starting from $\alpha = 2$ and up to $\alpha \rightarrow \infty$, the physical picture of the magnetization curve is as follows. At zero magnetic field the singlet ground state of the model consists of both basal and apical singlets. For very low magnetic fields $h \sim \alpha^{-2}$ the apical subsystem becomes partly polarized, while the basal subsystem remains in its singlet state. The magnetization of the apical subsystem smoothly increases with h and at some ‘apical saturation field’ $h_{low} \approx 0.26/\alpha^2$, the apical subsystem becomes fully polarized, $m = \frac{1}{2}$. Further increase of the magnetic field $h > h_{low}$ does not lead to the increase of the magnetization, providing a magnetization plateau at $m = \frac{1}{2}$, until the magnetic field overcomes the singlet-triplet gap of the basal subsystem $h_{up} = (\Delta_1 - \frac{1}{\alpha})$, at which the magnetization starts to increase from the plateau at $m = \frac{1}{2}$.

We compared the studied models with $s_a = s_b = \frac{1}{2}$ F-AF delta chain and found that the behavior of these systems is similar near the transition point. That is, the ground state magnetization in the vicinity of the critical point is slightly higher than the magnetization at the critical point, $m_c = s_a + s_b - \frac{1}{2}$. We believe that the latter fact is common for F-AF delta chains with any values of s_a and s_b .

The behavior of the models far from the critical point is very different. The ground state of the $s_a = s_b = \frac{1}{2}$ F-AF delta chain remains ferrimagnetic for all values of α , while the ground state of the studied models is singlet for large α . This difference stems from a different type of spectrum of basal AF chains: the gapped one for spin-1 and gapless for spin- $\frac{1}{2}$. The polarization of the apical subsystem induces a weak magnetic field acting on the basal subsystem, which results in a weak polarization of the basal subsystem for the

$s_a = s_b = \frac{1}{2}$ F-AF delta chain, which turns out to be energetically favorable. But for the studied model with $s_b = 1$ such a weak induced magnetic field can not overcome the finite singlet-triplet energy gap of the basal subsystem, which makes the polarization of the apical subsystem energetically unfavorable.

Acknowledgments

The numerical calculations were carried out with use of the ALPS libraries [37].

-
- [1] H. T. Diep (ed) 2013 Frustrated Spin Systems (Singapore; World Scientific).
 - [2] C. Lacroix, P. Mendels and F. Mila, eds., Introduction to frustrated magnetism. Materials, Experiments, Theory(Springer-Verlag, Berlin, 2011).
 - [3] O. Derzhko, J. Richter, M. Maksymenko, Int. J. Mod. Phys B **29**, 153007 (2015).
 - [4] M. Maksymenko, A. Honecker, R. Moessner, J. Richter, and O. Derzhko, Phys. Rev. Lett. **109**, 096404 (2012).
 - [5] J. Richter, O. Derzhko and J. Schulenburg, Phys. Rev. Lett. **93**, 107206 (2004).
 - [6] M. E. Zhitomirsky, H. Tsunetsugu, Phys. Rev. B **70**, 100403(R) (2004).
 - [7] M. E. Zhitomirsky and H. Tsunetsugu, Phys. Rev. B **75**, 224416 (2007).
 - [8] M.E. Zhitomirsky and H. Tsunetsugu, Progr. Theor. Phys. Suppl. **160**, 361 (2005).
 - [9] S. Capponi, O. Derzhko, A. Honecker, A.M. Lauchli, J. Richter, Phys. Rev. B **88**, 144416 (2013).
 - [10] J. Richter, O. Krupnitska, V. Balika, T. Krokhumalski, O. Derzhko, Phys. Rev. B **97**, 024405 (2018).
 - [11] A. Metavitsiadis, C. Psaroudaki, W. Brenig, Phys. Rev. B **101**, 235143 (2020).
 - [12] C. Ruiz-Perez, M. Hernandez-Molina, P. Lorenzo-Luis, F. Lloret, J. Cano, M. Julve M., Inorg. Chem., **39**, 3845 (2000).
 - [13] Y. Inagaki, Y. Narumi, K. Kindo, H. Kikuchi, T. Kamikawa, T. Kunimoto, S. Okubo, H. Ohta, Y. Saito, M. Azuma, M. Takano, H. Nojiri, M. Kaburagi, T. Tonegawa, J. Phys. Soc. Jpn., **74**, 2831 (2005).
 - [14] T. Tonegawa, M. Kaburagi, J. Magn. Magn. Mater., **272–276**, 898 (2004).

- [15] M. Kaburagi, T. Tonegawa, M. Kang, *J. Appl. Phys.*, **97**, 10B306 (2005).
- [16] R. Shirakami, H. Ueda, H. O. Jeschke, H. Nakano, S. Kobayashi, A. Matsuo, T. Sakai, N. Katayama, H. Sawa, K. Kindo, C. Michioka, K. Yoshimura, *Phys. Rev. B* **100**, 174401 (2019).
- [17] A. Baniodeh, N. Magnani, Y. Lan Y., G. Buth, C. E. Anson, J. Richter, M. Affronte, J. Schnack., A. K. Powell, *Npj Quant.Mater.* 2018. V. 3.1. P. 10.
- [18] V. Ya. Krivnov, D. V. Dmitriev, S. Nishimoto, S.-L. Drechsler, and J. Richter, *Phys. Rev. B* **90**, 014441 (2014).
- [19] D. V. Dmitriev, V. Ya. Krivnov, *Phys. Rev. B* **92**, 184422 (2015).
- [20] D. V. Dmitriev, V. Ya. Krivnov, *J. Phys.: Condens. Matter* **28**, 506002 (2016).
- [21] D. V. Dmitriev, V. Ya. Krivnov, J. Richter, J. Schnack, *Phys. Rev. B* **99**, 094410 (2019); *Phys. Rev. B* **101**, 054427 (2020).
- [22] O. Derzhko, J. Schnack, D. V. Dmitriev, V. Ya. Krivnov, J. Richter, *Eur. Phys. J. B* **93**, 161 (2020).
- [23] T. Yamaguchi, S.-L. Drechsler, Y. Ohta, S. Nishimoto, *Phys. Rev. B* **101**, 104407 (2020).
- [24] R. Rausch, M. Peschke, C. Plorin, J. Schnack, C. Karrasch, *SciPost. Phys.* **14**, 052 (2023).
- [25] B. Koteswararao, A. V. Mahajan, F. Bert, P. Mendels, J. Chakraborty, V. Singh, I. Dasgupta, S. Rayaprol, V. Siruguri, A. Hoser and S. D. Kaushik, *J. Phys.:Condens. Mat.* **24**, 236001 (2012).
- [26] O. S. Volkova, I. S. Maslova, R. Klingigiler, M. Abdrl-Hafiez, Y. C. Araugo, A. U. B. Wolter, V. Kataev, B. Buchner, and A. N. Vasiliev, *Phys. Rev. B* **85**, 104420 (2012).
- [27] S. E. Dutton, M. Kumar, Z. G. Soos, C. L. Broholm, and R. J. Cava, *J. Phys.: Condens. Mat.*, **24**, 166001 (2012).
- [28] T. Yamaguchi, Y. Ohta, & S. Nishimoto, *Phys. Rev. B*, **103**, 184410 (2021).
- [29] M. Takahashi, T. Sakai, *J. Phys. Soc. Jpn.***60**, 760 (1991).
- [30] E. S. Sorensen, I. Affleck, *Phys. Rev. Lett* **71**, 1633 (1993).
- [31] K. Okunishi, T. Hieida, Y. Akutsu, *Phys. Rev. B* **59**, 6806 (1999).
- [32] R. P. Hodgson, J. B. Parkinson, *J.Phys.C***18**, 6385 (1985).
- [33] H. Kiwata, Y. Akutsu, *J. Phys. Soc. Jpn.***63**, 3598 (1994).
- [34] S. R. White, *Phys. Rev. Lett.*, **69**, 2863 (1992).
- [35] V. Ravi Chandra, D. Sen, N. B. Ivanov, J. Richter, *Phys. Rev. B* **69**, 214406 (2004).
- [36] R. B. Griffiths, *Phys. Rev.* **A133**, 768 (1964).

[37] F. Alet et al., J. Phys. Soc. Jpn. Suppl. **74**, 30 (2005).